DOI 10.5162/sensoren2016/3.4.4

High Performance Current Measurement with Low-Cost Shunts by means of Dynamic Error Correction

Patrick Weßkamp[1], *Joachim Melbert*[1]
[1]*Ruhr-Universität Bochum, Forschungsgruppe Kfz-Elektronik, Universitätsstr. 150, ID 03/322, 44801 Bochum, Germany*

Abstract

Measurement of electrical current is often performed by using shunt resistors. Thermal effects due to self-heating and ambient temperature variation limit the achievable accuracy, especially if low-cost shunt resistors with increased temperature coefficient are utilized. In this work, a compensation method is presented which takes static and dynamic temperature drift effects into account and allows a correction of the measurement error. A thermal model of the shunt resistor setup is derived for this purpose and a suitable calibration method is developed. The correction algorithm is implemented in laboratory test equipment for long-term studies on automotive lithium-ion cells. For a 600 A current pulse, it reduces the measurement error from 2% to less than 0.1%. Measurements with a real-life testing profile show a reduction of remaining measurement error by 60%. The proposed dynamic error correction algorithm therefore allows high measurement accuracy despite the use of low-cost shunt resistors.

Keywords: Shunt resistor, calibration, error correction, thermal effects

Introduction

Measurement of electrical current is important for many scientific and industrial applications. One example is the growing number of hybrid and electrical vehicles, which require precise on-board measurement of current in the range of several hundreds of amperes for tracking the State-of-Charge (SoC) of the battery. In addition, preliminary testing of the automotive battery cells is necessary to determine the electrical behavior as a function of aging. Suitable laboratory equipment for this task has even higher demands on accuracy, bandwidth and noise of the current measurement. Frequencies of interest range from DC up to several ten kilohertz.
Suitable sensor concepts for these applications include shunt resistors and current transducers based on the Hall Effect or on the fluxgate measurement principle (Tab. 1). Although current transducers offer electrical isolation and negligible power losses, they are susceptible to magnetic stray fields and temperature-dependent offsets, add additional noise from the control electronics and have limited measurement bandwidth, depending on the sensor type. Their complexity also significantly increases the total system cost [1]. Shunt resistors therefore represent a low-cost alternative, especially if electrical isolation is not required and isolation amplifiers can be avoided. This is the case for single-cell battery test equipment [2].

Tab. 1: Comparison of current measurement techniques suitable from DC up to several ten kilohertz.

	Pro	Contra
Shunt	Low complexity, low cost, wide bandwidth	Power dissipation, no isolation, self-heating
Hall-Effect	Isolation, no power losses	temperature-dependent offset, limited accuracy
Flux-gate	Isolation, no power losses, good accuracy	Disturbance due to excitation frequency, large operation current, limited bandwidth w/o additional transformer, cost

The value of the shunt resistor has to be chosen with regard to signal range and power dissipation: The voltage drop across the shunt is typically in the range of several hundred mV in order to reduce the noise of the amplifier stage, to increase the effective resolution and to limit the influence of the thermoelectric effect. On the downside, the high currents used for automotive battery testing lead to significant power dissipation and self-heating of the shunt, resulting in a change of resistance described by the temperature coefficient α_{TK}. Without compensation, this

leads to increased measurement errors and uncertainty.
Straightforward solutions encompass the use of resistances with very low temperature coefficient, better cooling concepts or oversizing in terms of maximum power ratings, all of which might reduce the thermal effects below an acceptable threshold. In any case, these methods typically lead to increased material and space requirements as well as higher cost.
Direct compensation methods are an alternative approach and are known to improve the measurement accuracy: A temperature sensor measures the temperature of the shunt material and corrects the current measurement based on the known material characteristics [3].
However, this direct approach is limited if there is a thermal resistance between the shunt material and the location of the temperature sensor, for example if the resistance is enclosed in a package and the shunt material is not directly accessible. This is the case for nearly all available shunt resistors intended for heatsink mounting. In this situation, the inner shunt temperature cannot be measured directly and is typically higher than the sensor temperature. For the thermal steady state, the inner temperature still can be calculated if the thermal resistance is known [3].
Unfortunately, these static methods do not take into account the thermal capacitances of the materials along the path of the heat flow. As shown in the following sections, they lead to different dynamic behavior of shunt and sensor temperature and therefore induce time dependent measurement errors.
In this paper a method is presented to overcome these challenges and to provide a dynamic error correction procedure. With this method it is possible to calculate the inner shunt temperature also during arbitrary thermal transients and to dynamically compensate the temperature drift of a shunt resistor.

Current measurement for test equipment for automotive lithium-ion cells

For aging studies on automotive lithium-ion cells, specialized test equipment is necessary to cycle the cells with realistic currents and to measure small variations in the electrical behavior with high precision. Currents up to 600 A with frequencies from DC up to the kilohertz range are typical [2]. Due to the low voltage range of a single battery cell, electrical isolation is not required and shunt resistors can be used for current measurement. Their low cost compared to other solutions is advantageous for building a large number of test systems; additionally their wide bandwidth and inherent accuracy for low currents are also favorable (see Tab. 1).
The cell tester developed by our research group uses multiple 10 mΩ shunt resistors (TO-247 package) in parallel connection, mounted on a heatsink with water cooling. Electrical connection is accomplished by copper busbars. The overall resistance is approximately 1 mΩ, taking the resistance of the interconnection into account (Fig. 1).

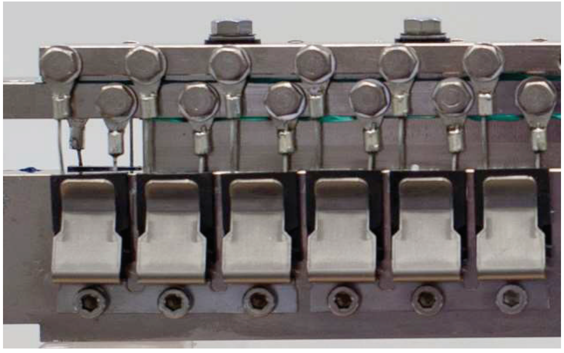

Fig. 1: 1 mΩ shunt resistor for lithium-ion cell test equipment, consisting of multiple 10 mΩ shunt resistances in TO-247 package mounted on a heatsink with water cooling.

For this application, the measurement error of the electrical current should be well below 0.1% for a wide current range in order to determine the capacity of lithium-ion cells by integration of the current flowing into the cell.

Shunt resistor: Temperature coefficient

For low currents this maximum error can easily be accomplished by periodic linear calibration and measurement of the actual shunt resistance, which eliminates any static errors due to resistance tolerances and slow drift effects over time.
However, a linear calibration technique cannot compensate the effect of the temperature coefficient of the shunt, which is determined to $\alpha_{TK} = 422\ \mathrm{ppm/K}$ from the measurement in Fig. 2. For the maximum current of 600 A the power dissipation is 25 W per resistor. Although this is sufficiently below the respective absolute maximum rating of 100 W, the thermal resistance of the shunt and the heatsink lead to an inner temperature rise of 30 °C, equivalent to a resistance variation of 1.5%. Without further compensation, the relative current measurement error has the same value and is an order of magnitude higher than desired.

DOI 10.5162/sensoren2016/3.4.4

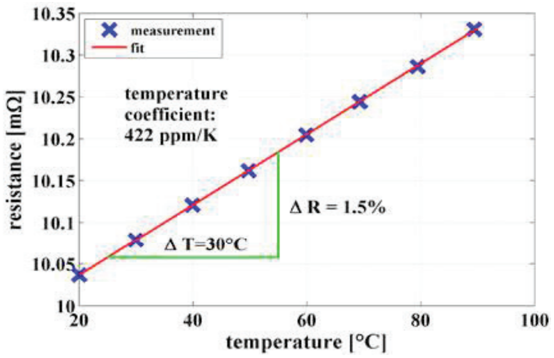

Fig. 2: Measured temperature dependence of a single 10 mΩ shunt resistor, approximated by a linear fit. The total resistance change for a temperature increase of ΔT=30 °C is highlighted [4].

In the shown configuration, the copper busbars and other interconnections also contribute a small part to the total shunt resistance (<10%) and to the overall temperature coefficient. Because the temperature coefficient of copper is quite high (~3900 ppm/K), the additional resistance increases the total temperature coefficient to $\alpha_{\mathrm{TK}} \approx 600\ \mathrm{ppm/K}$.
Temperature variation of the cooling water (or more generally of the ambient temperature) will also lead to a drift of the shunt resistance value and has to be taken into account.

Nonlinear calibration for thermal steady-state

The temperature dependence of the shunt resistance used in this work can be approximated with good concordance by a linear function, as demonstrated in Fig. 2, and is given by the equation

$$\begin{aligned} R(T) &= R_0\big(1+\alpha_{\mathrm{TK}}(T-T_0)\big) \\ &= R_0(1+\alpha_{\mathrm{TK}}\Delta T). \end{aligned} \tag{1}$$

Here, R_0 depicts the resistance value at the (arbitrary) temperature T_0. Typically, R_0 is measured during calibration and T_0 is set by the temperature during this procedure.
Two effects can lead to a temperature variation during operation: Self heating and ambient temperature change.

$$\Delta T = \Delta T_{\text{self-heating}} + \Delta T_{\mathrm{amb}}. \tag{2}$$

The ambient temperature rise is given by the difference between the present ambient temperature T_{amb} and the calibration temperature T_0:

$$\Delta T_{\mathrm{amb}} = T_{\mathrm{amb}} - T_0. \tag{3}$$

The self-heating is caused by the power dissipation P_{loss} in the resistance material due to the electrical current I. The associated temperature rise for the thermal steady-state is calculated using the total thermal resistance $R_{\mathrm{th,total}}$ between the resistor and the environment:

$$P_{\mathrm{loss}} = R(T)\, I^2 \tag{4}$$

$$\begin{aligned} \Delta T_{\text{self-heating}} &= R_{\mathrm{th,total}}\, P_{\mathrm{loss}} \\ &= R_{\mathrm{th,total}}\, R(T)\, I^2 \\ &\approx R_{\mathrm{th,total}}\, R_0\, I^2\,. \end{aligned} \tag{5}$$

The approximation made in the last step of Eq. (5) simplifies the following calculation. It can be shown that the overall calibration error associated with this assumption is below 0.04% and therefore can be disregarded.
Substituting Eq. (2) - (5) in Eq. (1) yields

$$\begin{aligned} R(I,\Delta T_{\mathrm{amb}}) = {} & R_0\big(1+\alpha_{\mathrm{TK}}\Delta T_{\mathrm{amb}} \\ & + \alpha_{TK} R_{\mathrm{th,total}} R_0\, I^2\big). \end{aligned} \tag{6}$$

This equation describes the resistance variation due to self-heating and ambient temperature change.
The shunt is used for current sensing by measuring the voltage drop over the resistor:

$$\begin{aligned} U_{\mathrm{shunt}} &= R(I,\Delta T_{\mathrm{amb}})\, I \\ &= R_0(1+\alpha_{\mathrm{TK}}\Delta T_{\mathrm{amb}})\, I \\ &\quad + \big(\alpha_{\mathrm{TK}} R_{\mathrm{th,total}} {R_0}^2\big)\, I^3 \\ &= a_1 I + a_3 I^3. \end{aligned} \tag{7}$$

As demonstrated in Eq. (7), the relationship between voltage and current is expressed by a polynomial function of degree 3, with a clear separation between effects due to self-heating ($\sim I^3$) and ambient temperature change ($\sim I$).
During calibration, a known reference current I_{ref} flows through the shunt resistor and the voltage is measured. Using polynomial curve fitting tools on the resulting data set for multiple current values, the parameters a_1 and a_3 can be determined. Note that this only works in the thermal steady-state, i.e. for each data point one has to wait until the measurement values do not change anymore.
The quality of the fit is demonstrated in Fig. 3 for an ambient temperature of $T_{\mathrm{amb}} = 20\ °C$, the error between fit and measurement is depicted in the lower graph. The hypothetical error if the effects due to self-heating were not included in the model is also shown.

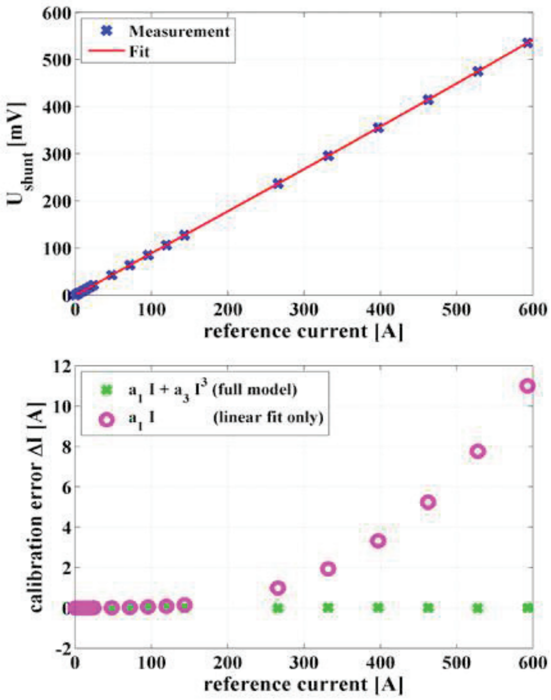

Fig. 3: Calibration measurement and resulting error for T_{amb}=20 °C and thermal steady-state. The error of the proposed nonlinear model is below 20 mA, whereas the error for the linear fit (without self-heating effects) exceeds 10 A.

In Tab. 2 the determined parameters from the polynomial curve fitting are given for two different ambient temperatures. As predicted by the theoretical approach, the values of a_3 are virtually independent of the ambient temperature rise and describe only effects due to self-heating. From the varying value of a_1 the resistance $R_0 = 0.8868\mathrm{m\Omega}$ (T_0=20°C) and the temperature coefficient $\alpha_{\mathrm{TK}} = 594\,\mathrm{ppm/K}$ can be determined. The overall thermal resistance is obtained from a_3 and equals $R_{\mathrm{th,total}} = 0.10\ \mathrm{K/W}$.

Tab. 2: Extracted parameters a_1 and a_3 using polynomial curve fitting for different ambient temperatures

	a_1 [µV/A]	a_3 [pV/A³]
T_{amb}=20 °C	886.77	46.683
T_{amb}=28 °C	890.85	46.685
Physical representation	Resistance and ambient temperature change	Self-heating

With knowledge of the parameters R_0, α_{TK} and a_3, equation (7) can be used to calculate the true current I from a measurement of the shunt voltage U_{shunt}. The ambient temperature T_{amb} also has to be known; it can either be measured by a temperature sensor or set to the typical operation condition.

Heat Flow and Thermal Modeling

The nonlinear calibration technique discussed in the previous section is only valid for the thermal steady-state, i.e. when the inner shunt temperature is constant and does not change anymore. Obviously, this also implies a constant electrical current *I* and sufficient settling time after a current step, typically in the range of several minutes. However, realistic testing procedures for lithium-ion cells require much faster current transients. The static calibration approach therefore has to be extended by a dynamic thermal model for this application.

The simplified structure in Fig. 4 is a sufficiently accurate approximation of the actual shunt resistor setup and is used for the derivation of the thermal model. It consists of a lumped shunt resistor and an optional temperature sensor, mounted on a common heatsink.

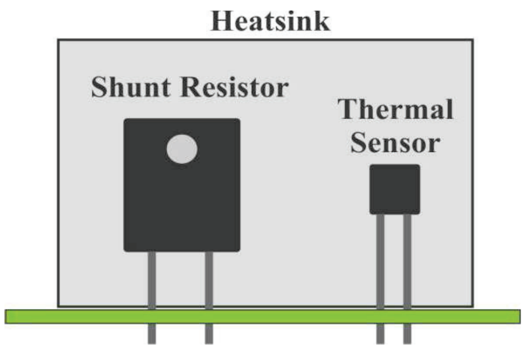

Fig. 4: Shunt resistor and temperature sensor mounted on a common heatsink (simplified structure)

Unfortunately, exact thermal modelling of the structure shown in Fig. 4 still is complicated and requires the use of simulation and the finite element method. The resulting thermal model is of high complexity and cannot be analyzed in real-time on an embedded system. More suitable for this application is a lumped element approach, consisting of a small number of thermal resistances and thermal capacitances.

The corresponding thermal model is given in Fig. 5 and was optimized empirically. The characteristics of the heat conduction are represented by an equivalent electrical circuit diagram, substituting temperature by voltage and heat flow by current [5]. Therefore, well-known methods for electrical circuit analysis can also be applied for thermal analysis.

The upper half of Fig. 5 describes the inner shunt temperature T_{shunt}. The total thermal resistance from Eq. (7) is split into four separate terms, so that $R_{\mathrm{th,total}} = R_{\mathrm{th,0}} + R_{\mathrm{th,1}} + R_{\mathrm{th,2}} + R_{\mathrm{th,3}}$, and thermal capacitances are added. They represent the dynamic behavior of the heat transfer through different materials between the inner shunt resistance and the heatsink.

The lower half of Fig. 5 describes the influence of the power dissipation P_{loss} on the optional temperature sensor. Ideally, the sensor would directly measure the ambient temperature T_{amb}, but usually some part of the heat generated by the shunt resistor is also coupled to the sensor, increasing T_{sensor}. This impacts the measurement of the true ambient temperature and needs to be taken into account.

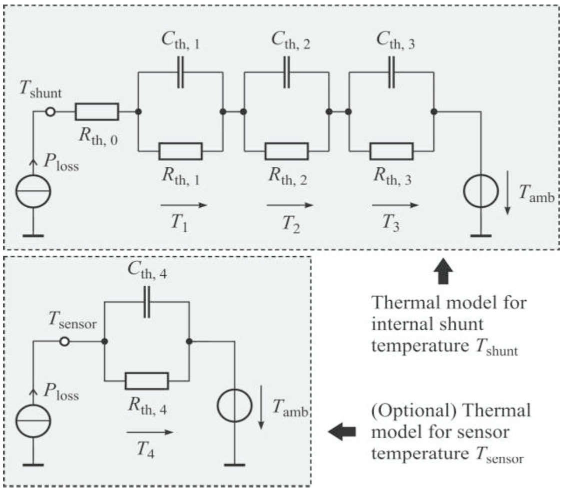

Fig. 5: Thermal model used for calculation of the internal shunt temperature and the variation of the sensor temperature due to self-heating

The chosen model structure (Foster network) simplifies the following calculations, but at the disadvantage of no direct physical equivalent of the lumped circuit elements, as explained in [6].

The analysis of the circuit is best done in the frequency domain, using the complexed valued thermal impedance $Z_{\mathrm{th}}(j\omega)$. For the upper circuit, the resulting equation is

$$T_{\mathrm{shunt}}(j\omega) = T_{\mathrm{amb}} + P_{\mathrm{loss}} R_{\mathrm{th,0}} + P_{\mathrm{loss}} \sum_{i=1}^{3} R_{\mathrm{th,i}} \frac{1}{1 + j\omega\tau_{\mathrm{i}}}. \tag{8}$$

The dynamic effects of self-heating therefore are given by the sum of three independent low-pass filters with time-constants $\tau_{\mathrm{i}} = R_{\mathrm{th,i}} C_{\mathrm{th,i}}$ and a time-invariant part due to $R_{\mathrm{th,0}}$.

Likewise, the transfer function for the sensor temperature can be obtained.

Dynamic parameter estimation

To parametrize the model from Fig. 5, a measurement of the shunt resistor voltage response $\Delta U_{\mathrm{shunt}}$ after a current step $\Delta\mathrm{I}$ (starting from $\mathrm{I} = 0$) is utilized. If the ambient temperature is held constant, according to Eq. (8) the change of the shunt temperature in time domain is equal to

$$\Delta T_{\mathrm{shunt}}(t) = \Delta P_{\mathrm{loss}} \Big(R_{\mathrm{th,0}} + \sum_{i=1}^{3} R_{\mathrm{th,i}} \big(1 - e^{-t/\tau_{\mathrm{i}}}\big) \Big). \tag{9}$$

With $\Delta P_{loss} = R_0 \Delta\mathrm{I}^2$, the resulting voltage change can be calculated from Eq. (1):

$$\begin{aligned} \Delta U_{\mathrm{shunt}}(\mathrm{t}) &= \alpha_{\mathrm{TK}} R_0 \,\Delta\mathrm{I}\, \Delta T_{\mathrm{shunt}}(t) \\ &= \alpha_{\mathrm{TK}} {R_0}^2 \Delta\mathrm{I}^3 \Big(R_{\mathrm{th,0}} + \sum_{i=1}^{3} R_{\mathrm{th,i}} \Big(1 - e^{-\frac{t}{\tau_{\mathrm{i}}}}\Big) \Big) \\ &= \alpha_{\mathrm{TK}} R_{\mathrm{th,total}} {R_0}^2 \Delta\mathrm{I}^3 \Big(\frac{R_{\mathrm{th,0}}}{R_{\mathrm{th,total}}} + \sum_{i=1}^{3} \frac{R_{\mathrm{th,i}}}{R_{\mathrm{th,total}}} \Big(1 - e^{-\frac{t}{\tau_{\mathrm{i}}}}\Big) \Big). \end{aligned} \tag{10}$$

Note that the factor $a_3 = \alpha_{\mathrm{TK}} R_{\mathrm{th,total}} {R_0}^2$ already has been obtained from the steady-state calibration. The dynamic behavior therefore is fully characterized by measuring the time constants τ_{i} and the *ratio* of the associated amplitude factors $R_{\mathrm{th,i}} / R_{\mathrm{th,total}}$ (the sum of all ratios is equal to one).

The identification of these parameters is accomplished by nonlinear curve fitting techniques and is shown in Fig. 6.

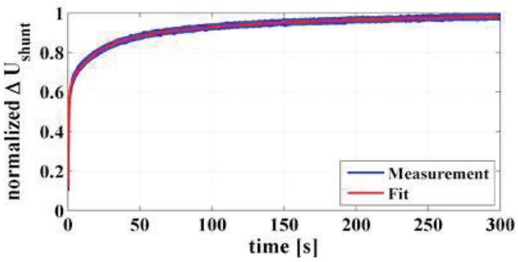

Fig. 6: Normalized change of shunt voltage due to self-heating after a current step

Tab. 3: Extracted parameters for the thermal model due to self-heating

	i=0	i=1	i=2	i=3
$R_{\mathrm{th,i}}$ / $R_{\mathrm{th,total}}$	0.11	0.52	0.21	0.15
τ_{i} [s]	-	0.67	16.82	107.8

For the thermal model of the temperature sensor, a similar technique is used for

DOI 10.5162/sensoren2016/3.4.4

parameter identification, yielding values for $R_{th,4}$ and $C_{th,4}$.

Dynamic error correction procedure

The static and dynamic knowledge of the system are used to develop a dynamic error correction procedure for the current measurement. First, Eq. (7) is solved for the unknown current I:

$$\begin{aligned} U_{\text{shunt}} &= a_1 I + a_3 I^3 \\ &= (a_1 + a_3 I^2) I \end{aligned} \quad (7)$$

$$\begin{aligned} \Leftrightarrow \; I &= \frac{U_{\text{shunt}}}{a_1 + a_3 I^2} \\ &= \frac{U_{\text{shunt}}}{R_0(1 + \alpha_{\text{TK}} \Delta T_{\text{amb}}) + a_3 \underbrace{I^2}_{h(t)*I^2(t)}} \end{aligned} \quad (11)$$

As previously explained, the term $a_3 I^2$ describes the effects due to self-heating in thermal steady-state. The dynamic properties of the thermal model in Fig. 5 are included in this equation by replacing I^2 with the output of a dynamic filter, whose impulse response is given by $h(t)$. The filter output is mathematically described by the convolution $h(t) * I^2(t)$ in the time domain.
The corresponding transfer function $H(j\omega)$ of the filter in the frequency domain is derived from Eq. (8), omitting the ambient temperature and normalizing the factors:

$$H(j\omega) = \frac{R_{\text{th,0}}}{R_{\text{th,total}}} + \sum_{i=1}^{3} \frac{R_{\text{th,i}}}{R_{\text{th,total}}} \frac{1}{1 + j\omega\tau_{\text{i}}}. \quad (12)$$

For a practical implementation of the correction algorithm, equations (11) and (12) are both transformed to discrete-time representations with a fixed time step. The filter then is easily implemented by three first order IIR-filter structures on a microcontroller. Additionally, the input $I^2(t)$ required by the dynamic model can be approximated by the value from the previous time-step, i.e. $I^2(t) \approx I^2(t - \Delta t)$.
For the thermal model of the temperature sensor (lower part of Fig. 5) the same approach is used, yielding a mathematical expression for the temperature change of the sensor due to self-heating of the shunt. Subtracting this value from the measured sensor value yields a good approximation of the true ambient temperature T_{amb}.
A graphical illustration of the overall algorithm is given in Fig. 7.

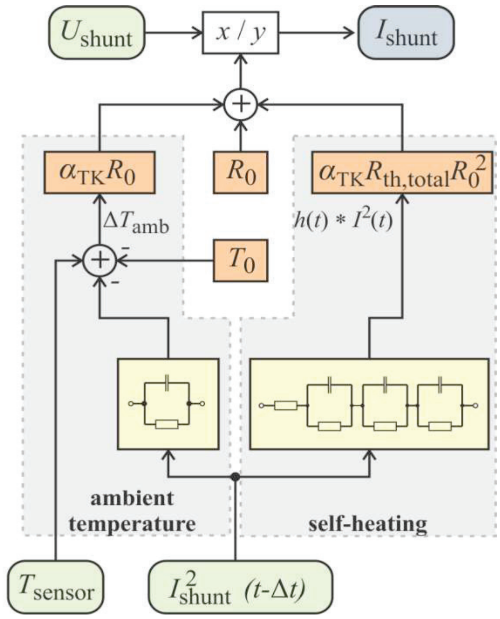

Fig. 7: Overall dynamic correction algorithm, taking into account effects due to self-heating and ambient temperature change

Measurement Results

The performance of the proposed algorithm is demonstrated in Fig. 8 for a 600 A constant-current pulse. The new dynamic compensation scheme reduces the relative measurement error from 2% (no temperature compensation) to less than 0.1% after 2 s settling time. For comparison, the steady-state compensation without dynamic effects requires 180s to reach this band of error.

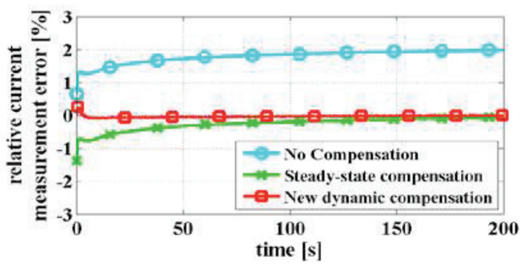

Fig. 8: Relative current measurement error after a current step at t = 0 s from 0 A to 600 A for different temperature compensation schemes.

In order to demonstrate the real-life improvement factor of the algorithm, a realistic testing profile for automotive Li-Ion cells is evaluated in Fig. 9. The resulting relative current measurement error is depicted in the lower graph for an excerpt from the profile. For low currents, the thermal effects are negligible and there is no difference between the compensation schemes. For higher currents the error increases significantly, if no compensation or only steady-state compensation is used. In comparison, the proposed transient correction algorithm is able to keep the measurement error within a small band of error.

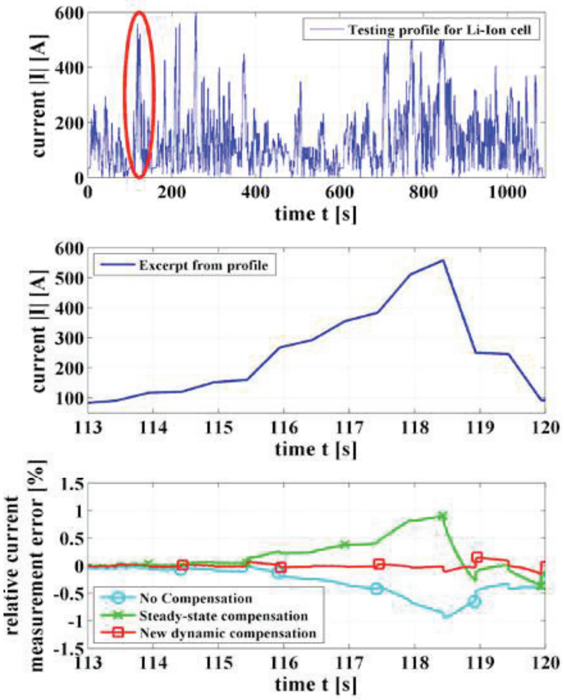

Fig. 9: Realistic testing profile for Lithium-Ion cells and associated relative current measurement errors.

The arithmetic mean of the relative current measurement error given in Tab. 4 for the complete testing profile is a measure for the real-life improvement factor. For the shown profile, the dynamic algorithm reduces the mean error by 60% compared to the case if no temperature compensation is used, and by 40% compared to the steady-state only calibration.

Tab. 4: Arithmetic mean of the relative current measurement error calculated for the complete testing profile given in Fig. 9.

Compensation algorithm	**Mean measurement error**
No compensation	0.211%
Steady-State only	0.139%
New dynamic method	0.085%

Summary and Conclusions

In this paper, a dynamic error compensation procedure is presented, which is able to correct the current measurement errors of shunt resistors due to self-heating and ambient temperature change. The method is based on a theoretical analysis of the shunt resistance variation due to temperature change for thermal steady-state. It is supplemented by a dynamic model describing transient thermal effects due to self-heating and heat-transfer over a heatsink. A temperature sensor in combination with a correction algorithm is used to measure the true ambient temperature, independent of self-heating effects.

The proposed algorithm is used for current measurement in test-equipment for automotive lithium-ion cells employing low-cost shunt resistors. It is able to reduce the relative current measurement error from over 2% to less than 0.1% for a 600 A current pulse. For a real-life, dynamic testing profile the mean current measurement error is reduced by 60%.

The presented dynamic error correction procedure therefore enables precise current measurement with low-cost shunt resistors. It can be implemented in a microcontroller with low demands on computation power. If the ambient temperature does not change or is already known, the optional temperature sensor is not needed. Therefore, the algorithm can also be used to increase the accuracy of existing systems without the need for additional hardware components.

References

[1] S. Ziegler, R. C. Woodward, H. H.-C. Iu, and L. J. Borle, “Current Sensing Techniques: A Review,” *IEEE Sensors J,* vol. 9, no. 4, pp. 354–376, 2009; doi: 10.1109/JSEN.2009.2013914

[2] N. Lohmann, P. Weßkamp, P. Haußmann, J. Melbert, and T. Musch, “Electrochemical impedance spectroscopy for lithium-ion cells: Test equipment and procedures for aging and fast characterization in time and frequency domain,” *Journal of Power Sources*, vol. 273, pp. 613–623, 2015; doi: 10.1016/j.jpowsour.2014.09.132

[3] S. Ziegler, R. C. Woodward, H. H.-C. Iu, and L. J. Borle, “Investigation Into Static and Dynamic Performance of the Copper Trace Current Sense Method,” *IEEE Sensors J,* vol. 9, no. 7, pp. 782–792, 2009; doi: 10.1109/JSEN.2009.2021803

[4] E. Grundkötter, “Untersuchung des transienten thermischen Verhaltens von Shuntwiderständen zur Strommessung und Optimierung von Fehlerkorrekturverfahren,” Masterarbeit, Ruhr-Universität Bochum, Bochum, 2016.

[5] M. März and P. Nance, “Thermal Modeling of Power-electronic Systems,” Fraunhofer Institute for integrated circuits IIS-B, Erlangen, 2000.

[6] P. E. Bagnoli, C. Casarosa, M. Ciampi, and E. Dallago, “Thermal resistance analysis by induced transient (TRAIT) method for power electronic devices thermal characterization. I. Fundamentals and theory,” *IEEE Trans. Power Electron,* vol. 13, no. 6, pp. 1208–1219, 1998; doi: 10.1109/63.728348